Sergei D. Liazhkov

Unsteady thermal transport in an instantly heated semi-infinite free end Hooke chain

Abstract We consider unsteady ballistic heat transport in a semi-infinite Hooke chain with free end and arbitrary initial temperature profile. An analytical description of the evolution of the kinetic temperature is proposed in both discrete (exact) and continuum (approximate) formulations. By comparison of the discrete and continuum descriptions of kinetic temperature field, we reveal some restrictions to the latter. Specifically, the far-field kinetic temperature is well described by the continuum solution, which, however, deviates near and at the free end (boundary). We show analytically that, after thermal wave reflects from the boundary, the discrete solution for the kinetic temperature undergoes a jump near the free end. A comparison of the descriptions of heat propagation in the semi-infinite and infinite Hooke chains is presented. Results of the current paper are expected to provide insight into non-stationary heat transport in the semi-infinite lattices.

Keywords Ballistic heat transport · Kinetic temperature · Semi-infinite chain · Discrete solution · Continuum solution

1 Introduction

Heat transfer at the macroscale is known to be diffusive and to obey the Fourier law. Using of the law as a constitutive relation, a wide class of problems in continuum mechanics can be solved (see, e.g., [1]). However, theoretical studies [2–4] and experiments [5–11] show that at the micro- and nanoscale heat propagation is non-diffusive, e.g., ballistic. In particular, deviations from the Fourier law are demonstrated in nanotubes [5], silicon membranes [7], silicon nanowires [8,9] and graphene [11]. Therefore, building of theories, describing thermal processes at the micro- and nanoscale, is required and is relevant also for the reason of innovative development of micro- and nanoelectronics (see, e.g., [12–16]).

To the best of our knowledge, two approaches are used in general for the analytical description of heat transfer at the microscale (or nanoscale), namely the lattice dynamics (LD) approach and the kinetic theory. By dint of investigation of the Boltzmann transport equation (BTE), one can solve problems, which are unsolvable by the LD method (see, e.g., [17–19]). Since the BTE is continuum, quantities, obtained through BTE, change in space also continuously. Therefore, there may be some restrictions on description of heat transport at the

S. D. Liazhkov (✉)
Peter the Great Saint-Petersburg Polytechnic University, Politekhnicheskaya str. 29, St. Petersburg 195251, Russia
E-mail: sergeiliazhkov@gmail.com

S. D. Liazhkov
Institute for Problems in Mechanical Engineering of the Russian Academy of Sciences, Bol'shoy pr. 61, V.O., St. Petersburg 199178, Russia

nanoscale, where one may have necessity to deal with discrete structures. Hence, a question arises what these restrictions are.

In paper [20], the kinetic theory of unsteady heat transport in the infinite one-dimensional harmonic chain is linked with the LD theory. The approximate solution for the kinetic temperature is derived in the continuum limit using the discrete[1] (exact) solution, obtained by the LD approach. It is shown that the result is in a practically ideal agreement with the kinetic theory. Nonetheless, it remains still unclear whether the continuum solution, obtained by one or another method, corresponds to the exact one always.

In general, one can distinguish discrete and continuum analytical descriptions of the ballistic heat transport. In the pioneering work of Klein and Ilya Prigogine [21], the evolution law of the discrete field of the kinetic temperature was obtained using exact Schrödinger solution [22][2] of the dynamical equations for the Hooke chain[3]. The result was reproduced by Hemmer in his PhD thesis [25]. In the pioneering work by Krivtsov [26], the PDE for the continuum field of the kinetic temperature was derived, solution of which is proposed in the integral form. In papers [27,28], the discrete and continuum descriptions of kinetic temperature fields are compared. It is shown in [27] that the evolution over time of the kinetic temperature fields caused by arbitrary initial perturbation (except point) leads to indistinguishability of these. However, aforesaid results are about energy propagation in the *infinite* chains only.

The question of heat transport in the finite or semi-infinite lattices remains open. Some analytical treatments to describe it are proposed in studies [29,30]. In paper [29], the solution for the kinetic temperature in the finite[4] Hooke chain was obtained. Gudimenko [30] found approximate solution of heat transfer problem in the semi-infinite chain with an absorbing boundary. Despite the obtained results, many ambiguities remain, for instance, behavior of quantities at the boundary or influence of other boundary conditions on heat propagation. In particular, answering aforementioned problems, related to free boundaries, is necessary for development of theoretical models of the experiments associated, e.g., with reflection of phonons [31–33].

In this paper, we describe the process of heat transport in the semi-infinite free end Hooke chain. Firstly, we derive the exact solution for the kinetic temperature, and, following [20], we perform an approximation of it in the continuum limit. Then, analogously to [27,28], we compare the discrete (exact) and continuum descriptions of the heat transport. By the comparison, we reveal discrepancies between these descriptions near and at the boundary.

The paper is organized as follows. In Sect. 2, we formulate the problem and derive exact expression for particle velocities (Sect. 2.1), which is further applied to derive the exact expression for the kinetic temperature (Sect. 2.2). In Sect. 3, we determine the kinetic temperature in the continuum limit. In Sect. 4, the fundamental solution for the kinetic temperature in the continuum limit is derived, which is present as a sum of the contributions from incident and reflected thermal waves. We reveal an interrelation between the continuum solutions for the kinetic temperature in the semi-infinite and infinite Hooke chains. In Sect. 5, the discrete and continuum solutions for kinetic temperature fields are compared. Examples of the rectangular (Sect. 5.1) and step (Sect. 5.2) initial perturbations are considered. In Sect. 6, we compare the theory of ballistic heat transport in the semi-infinite and infinite Hooke chains and find an interrelation between the corresponding discrete solutions for the kinetic temperature. In Sect. 7, results of the paper are discussed.

2 Discrete solution for the kinetic temperature

2.1 Formulation of the problem and derivation of expression for particle velocities

We consider the semi-infinite Hooke chain[5], having one free end and assume that the particles of the chain interact with the nearest neighbors. Therefore, the dynamical equations can be written as

$$
\begin{aligned}
&\dot{u}_n = v_n, \\
&\dot{v}_0 = \omega_e^2(u_1 - u_0), \\
&\dot{v}_n = \omega_e^2(u_{n+1} - 2u_n + u_{n-1}), \quad n \in \mathbb{N}, \quad \omega_e = \sqrt{c/m},
\end{aligned}
\tag{1}
$$

---

[1] i.e., changing in dependence of the particle number.

[2] See also English translation of the Schrödinger article [23].

[3] This is the monoatomic harmonic chain of identical particles, connected by the linear identical springs, see [24].

[4] Ends of chain are connected with the fixed points by linear stiffness springs.

[5] Definition of the Hooke chain is given in Sect. 1 and in [24].

where m is the particle mass; c is the spring stiffness; and u_n and v_n are displacement and velocity of particle n, respectively. The equations are supplemented by the following initial conditions:

$$u_n = 0, \quad v_n = \mathcal{V}_n. \tag{2}$$

Here, $\mathcal{V}_n$ is the initial velocity field such that

$$\mathcal{V}_n = \rho_n \sqrt{\frac{k_{\mathrm{B}} T_n^0}{m}}, \tag{3}$$

where k_{B} is the Boltzmann constant; T_n^0 is the initial kinetic temperature of particle (see definition 5); ρ_n are uncorrelated random numbers with zero mean and unit variance:

$$\langle \rho_n \rangle = 0, \qquad \langle \rho_j \rho_n \rangle = \delta_{jn}, \tag{4}$$

where δ_{jn} is the Kronecker delta and $\langle ... \rangle$ stands for the mathematical expectation sign. Therefore, the initial conditions (2) with (3) and (4) imply an existence of some initial temperature field in the chain and zero initial heat fluxes[6] [26].

In order to define the kinetic temperature in the chain, we introduce an infinite set of realizations with different initial conditions (2). For the one-dimensional Hooke chain, we determine the kinetic temperature, T_n, as follows:[7]

$$m \langle v_n^2 \rangle \overset{\mathrm{def}}{=} k_{\mathrm{B}} T_n. \tag{5}$$

In general, two approaches are followed to obtain the kinetic temperature in the harmonic crystals. The first involves introducing of covariances of particle displacements and velocities and transformation of the stochastic dynamical equations to the deterministic PDE with respect to these covariances. This approach is extensively studied in, e.g., [26,38–40]. The second approach is to substitute exact expression for particle velocity into (5). One possible way to solve Eq. (1) analytically is to reformulate the dynamical problem for the finite chain with two free ends, exact solution of which is known [25,41] and then to proceed to the thermodynamic limit. The second way, based on operating of the difference equations, is described in [42,43]. However, these ways are harder than one, which is proposed below.

We introduce the direct and inverse discrete cosine transforms (DCT) as follows [44]:

$$\hat{u}(\theta) = \sum_{n=0}^{\infty} u_n \cos \frac{(2n+1)\theta}{2}, \quad u_n = \frac{1}{\pi} \int_{-\pi}^{\pi} \hat{u}(\theta) \cos \frac{(2n+1)\theta}{2} \, d\theta, \tag{6}$$

where θ is the wave number and $\hat{u}$ is some time-dependent function. Note that representation for the particle displacement (6) satisfies free boundary condition. Applying DCT (6) to Eqs. (1–2) yields equation

$$\ddot{\hat{u}} + \omega^2 \hat{u} = 0, \quad \omega(\theta) = 2\omega_e \left| \sin \frac{\theta}{2} \right|, \tag{7}$$

where ω is the dispersion relation for the Hooke chain, with the initial conditions

$$\hat{u} = 0, \quad \dot{\hat{u}} = \sum_{n=0}^{\infty} \mathcal{V}_n \cos \frac{(2n+1)\theta}{2}, \tag{8}$$

whence

$$\hat{u} = \frac{\sin(\omega t)}{\omega} \sum_{n=0}^{\infty} \mathcal{V}_n \cos \frac{(2n+1)\theta}{2}. \tag{9}$$

---

[6] The statement of problem corresponds to experimental heating of the crystal by the ultrashort laser pulse. Since the expression for heat flux in the Hooke chain contains covariances of displacements and velocities (see, e.g., [3,34]), initial zero field of initial displacements means zero initial heat fluxes.

[7] We determine the kinetic temperature by its statistical definition (see, e.g., chapter 3, Sect. 29 in [35]). Unambiguous definition of the temperature for systems far from equilibrium is still unresolved fundamental problem (see, e.g., [36,37]). In this paper, we calculate the kinetic temperature as average of kinetic energy over realizations, because it has simple physical meaning. Discussion of the ergodicity remains out of frameworks of this study.

Note that the dispersion relations for the semi-infinite and infinite chains coincide. Applying the inverse DCT to (9) with subsequent differentiation with respect to time gives the following equation for the particle velocity:

$$v_n = \frac{1}{\pi} \sum_{j=0}^{\infty} \mathcal{V}_j \int_{-\pi}^{\pi} \cos \frac{(2j+1)\theta}{2} \cos \frac{(2n+1)\theta}{2} \cos(\omega(\theta)t) \mathrm{d}\theta. \tag{10}$$

Thus, we have the exact expression for velocity of each particle in the semi-infinite chain. In the next subsection, Eq. (10) is employed to obtain the kinetic temperature.

2.2 Exact expression for the kinetic temperature

Substitution of the solution for particle velocity (10) to (5) using uncorrelatedness of the initial velocity field (4) and (3) yields

$$T_n = \frac{1}{\pi^2} \sum_{j=0}^{\infty} T_j^0 \left(\int_{-\pi}^{\pi} \cos \frac{(2j+1)\theta}{2} \cos \frac{(2n+1)\theta}{2} \cos(\omega(\theta)t) \mathrm{d}\theta \right)^2. \tag{11}$$

Equation (11) is the exact solution for the kinetic temperature in the semi-infinite chain with free end and will be further referred to as the *discrete solution*. Recall that the discrete solution for kinetic temperature in the *infinite* Hooke chain has the form [21,25,27]

$$T_{\inf n} = \sum_{j=-\infty}^{\infty} T_j^0 J_{2(n-j)}^2 (2\omega_e t), \tag{12}$$

where J is the Bessel function of the first kind. From comparison of Eqs. (11) and (12), it follows that equation for the discrete solution for kinetic temperature in the Hooke chain with arbitrary boundary conditions can be constructed as

$$T_n = \sum_{j\in\mathbb{P}} T_j^0 \left(\frac{\dot{\Phi}_{nj}(t)}{\omega_e} \right)^2, \tag{13}$$

where $\Phi_{nj}(t)$ is the solution of the equation

$$\ddot{\Phi}_n - \omega_e^2 \mathcal{L}_n \Phi_n = \omega_e \delta(t) \delta_{nj}, \quad n \in \mathbb{P}, \tag{14}$$

where $\mathcal{L}_n$ is the linear difference operator, which depends on specific boundary conditions; $\delta(t)$ is the Dirac delta function; $\mathbb{P}$ is set of numbers, by which particles in the system are indexed. The function Φ_n is supplemented by the initial condition [45]:

$$\Phi_n|_{t<0} = 0. \tag{15}$$

Equation (11) is further employed to obtain the kinetic temperature in the continuum limit.

3 Kinetic temperature in the continuum limit

In the section, we derive the kinetic temperature in the continuum limit, namely as a function of the continuum coordinate, x. This representation is suitable for general case when expression (11) becomes hard to use. We show that kinetic temperature in the continuum limit can be expressed as

$$T(x,t) = T^F(x,t) + T^S(x,t),$$
$$T^F = \frac{T^0(x)}{2} J_0(4\omega_e t), \quad T^S = \frac{1}{2\pi} \int_0^{\pi} T^0(|x + v_s t \cos\theta|) \mathrm{d}\theta, \tag{16}$$

where $v_s \overset{\text{def}}{=} \omega_e a$ is the speed of sound; a is the equilibrium distance (length of undeformed bond between particles); $T^0(x)$ is the continuum field of the kinetic temperature such that $T^0(an) = T_n^0$ (see derivation for details). We further refer (16) to as the *continuum solution*. Derivation of Eq. (16) is given below.
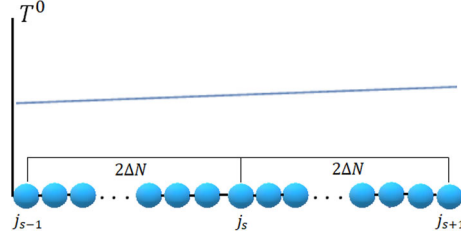
Fig. 1 Initial temperature profile

3.1 Continualization

We use an approach, proposed in paper [20]. First of all, we separate Eq. (11) into two terms, corresponding to the two physical processes:

$$
\begin{aligned}
T_n &= T_n^F + T_n^S, \\
T_n^F &= \sum_{j=0}^{\infty} T_j^0 F_{nj}, \quad T_n^S = \sum_{j=0}^{\infty} T_j^0 S_{nj}, \\
F_{nj} &= \frac{1}{2\pi^2} \iint_{-\pi}^{\pi} \cos \frac{(2j+1)\theta_1}{2} \cos \frac{(2j+1)\theta_2}{2} \cos \frac{(2n+1)\theta_1}{2} \\
&\quad \times \cos \frac{(2n+1)\theta_2}{2} \cos \left((\omega(\theta_1) + \omega(\theta_2)) t \right) d\theta_1 d\theta_2, \\
S_{nj} &= \frac{1}{2\pi^2} \iint_{-\pi}^{\pi} \cos \frac{(2j+1)\theta_1}{2} \cos \frac{(2j+1)\theta_2}{2} \cos \frac{(2n+1)\theta_1}{2} \\
&\quad \times \cos \frac{(2n+1)\theta_2}{2} \cos \left((\omega(\theta_1) - \omega(\theta_2)) t \right) d\theta_1 d\theta_2.
\end{aligned}
\tag{17}
$$

We further show that the first term corresponds to high-frequency oscillations of the kinetic temperature, caused by equilibration of the kinetic and potential energies [38]. This is a fast process, occurring in time of order of several hundreds atomic periods. The second term corresponds to the slow process caused by ballistic heat transport. Characteristic time scale of this process is much larger than one of the thermal equilibration. Following [20], we perform a continualization for the *slow* and *fast* terms of the kinetic temperature, T^S and T^F, respectively.

We introduce a mesoscale, which is larger than the distance between particles, a, but smaller than macroscale,[8] $\mathcal{A}$, and divide the chain into the equal intervals, indexed by s. Each interval s has the length $2a\Delta N$, $\Delta N \gg 1$, $a\Delta N \ll \mathcal{A}$ and is limited by the boundary particles, j_s. We assume that the initial temperature profile, enclosed in the intervals s, changes slowly (Fig. 1). Therefore, the length of the mesoscale is $2a\Delta N$. Then, the expression for T_n^S in (17) can be rewritten as

$$
\begin{aligned}
T_n^S &= \sum_{s=0}^{\infty} \sum_{j=j_s-\Delta N+1}^{j_s+\Delta N} T_j^0 S_{nj} \approx \sum_{s=0}^{\infty} T_{j_s}^0 \sum_{j=j_s-\Delta N+1}^{j_s+\Delta N} S_{nj} \\
&= 2a\Delta N \sum_{s=0}^{\infty} T_{j_s}^0 g_{n,j_s}^S(\Delta N), \quad g_{n,j_s}^S(\Delta N) = \frac{1}{2a\Delta N} \sum_{j=j_s-\Delta N+1}^{j_s+\Delta N} S_{nj},
\end{aligned}
\tag{18}
$$

where $g_{n,j_s}(\Delta N)$ determines contribution of the point j_s to the kinetic temperature at point n. Expression (18) is also valid for T^F if we replace S by F. It can also be interpreted as a discrete analogue of the fundamental solution, obtained by averaging of T_n over the mesoscale. Further, we derive the continuum fundamental solutions, corresponding to the slow term, g^S (see Sect. 3.2), and to the fast term, g^F (see Sect. 3.3).

---

[8] A macroscale can be interpreted as a scale of the order of the length of chain.

3.2 Slow term

The following expression for $g^S_{n,j_s}(\Delta N)$ is calculated up to the order $O\left(\frac{1}{\Delta N}\right)$ (see Appendix A) and is represented as follows:

$$g^S_{n,j_s}(\Delta N) \approx \frac{1}{16\pi^2 a} \iint_{-\pi}^{\pi} \left[\cos\left(\Delta\theta\omega'(\theta_1)t\right)\left[\cos((n+j_s)\Delta\theta) + \cos((n-j_s)\Delta\theta)\right.\right.$$
$$\left.\left. + \cos\left(\theta_1(2n+1) - (n+j_s)\Delta\theta\right) + \cos\left(\theta_1(2n+1) - (n-j_s)\Delta\theta\right)\right]\text{sinc}(\Delta N\Delta\theta) \right]d\theta_1 d\theta_2, \tag{19}$$

where $\Delta\theta = \theta_1 - \theta_2$, $()' = \frac{\mathrm{d}}{\mathrm{d}\theta_1}$, $\text{sinc}(x) = \dfrac{\sin x}{x}$. We change the variables $\theta = \theta_1$, $q = \Delta\theta$ and rewrite (19), using trigonometric identities and symmetry of the integrands with respect to zero:

$$g^S_{n,j_s}(\Delta N) \approx \frac{1}{4\pi} \int_0^{\pi} \left[\cos^2\frac{(2n+1)\theta}{2}\left[\psi_1(n+j_s+\omega'(\theta)t) + \psi_1(n+j_s-\omega'(\theta)t)\right.\right.$$
$$\left. + \psi_1(n-j_s+\omega'(\theta)t) + \psi_1(n-j_s-\omega'(\theta)t)\right]$$
$$+ \frac{\sin((2n+1)\theta)}{2}\left[\psi_2(n+j_s+\omega'(\theta)t) + \psi_2(n+j_s-\omega'(\theta)t)\right.$$
$$\left.\left. + \psi_2(n-j_s+\omega'(\theta)t) + \psi_2(n-j_s-\omega'(\theta)t)\right]\right]d\theta,$$
$$\psi_1(\Xi) = \frac{1}{2\pi a}\int_{\theta-\pi}^{\theta+\pi} \cos(\Xi q)\text{sinc}(q\Delta N)\mathrm{d}q,$$
$$\psi_2(\Xi) = \frac{1}{2\pi a}\int_{\theta-\pi}^{\theta+\pi} \sin(\Xi q)\text{sinc}(q\Delta N)\mathrm{d}q, \tag{20}$$

where ψ_1 and ψ_2 are referred to as wave packets propagating with group velocity $v_g = a\omega'$. Averaging of the function g^S_{n,j_s} over the mesoscale leads to a sum of the integrals of these wave packets. In the limit case $(\Delta N \gg 1)$, the wave packet ψ_2 is negligible and the expression for ψ_1 has the following approximate form (see Appendix B):

$$\psi_1(\Xi) \approx \frac{1}{2a\Delta N} H\left(1 - \frac{|\Xi|}{\Delta N}\right), \tag{21}$$

where $H(x)$ is the Heaviside function. Taking into account $\Delta N \gg 1$, we obtain the final form of the discrete fundamental solution:

$$g^S_{n,j_s}(\Delta N) \approx \frac{1}{4\pi}\int_0^{\pi}\left[\psi(n-j_s+\omega'(\theta)t, \Delta N) + \psi(n-j_s-\omega'(\theta)t, \Delta N)\right.$$
$$\left. + \psi(n+j_s+\omega'(\theta)t, \Delta N) + \psi(n+j_s-\omega'(\theta)t, \Delta N)\right]d\theta, \tag{22}$$
$$\psi(\Xi, \Delta N) = \frac{1}{2a\Delta N}\cos^2\left(\frac{\theta(2n+1)}{2}\right)H\left(1 - \frac{|\Xi|}{\Delta N}\right).$$

We introduce continuous functions $T^S(x)$, $T^0(x)$, $g^S_c(x, y)$ such that

$$T^0(an) = T^0_n, \quad g^S_c(x, y) = \lim_{\frac{a\Delta N}{\mathcal{A}} \to 0} g^S_{n,j_s}(\Delta N),$$
$$T^S(x) = \lim_{\frac{a\Delta N}{\mathcal{A}} \to 0} T^S_n = \int_0^{\infty} T^0(y)g^S_c(x, y)\mathrm{d}y. \tag{23}$$

In the limit case $a\Delta N/\mathcal{A} \to 0$, the function ψ can be replaced by the Dirac delta function. Using Eqs. (22) and (23), we obtain the fundamental solution for the slow term of the kinetic temperature:

$$g^S_c(x, y) = g^S(x - y) + g^S(x + y),$$
$$g^S(x) = \frac{1}{4\pi}\int_0^{\pi}\left[\delta(x + v_g(\theta)t) + \delta(x - v_g(\theta)t)\right]d\theta, \tag{24}$$

where $v_g(\theta) = v_s \cos \dfrac{\theta}{2} \, \text{sgn} \left(\sin \dfrac{\theta}{2} \right)$ is the group velocity.[9]

The slow term T^S is further obtained as the integral convolution of this fundamental solution with field of the initial temperature:

$$T^S = \frac{1}{4\pi} \int_0^\infty T^0(y) \left[\int_0^\pi \delta(x - y + v_g(\theta)t) \, \mathrm{d}\theta + \int_0^\pi \delta(x - y - v_g(\theta)t) \, \mathrm{d}\theta \right. \\ \left. + \int_0^\pi \delta(x + y - v_g(\theta)t) \, \mathrm{d}\theta + \int_0^\pi \delta(x + y + v_g(\theta)t) \, \mathrm{d}\theta \right] \mathrm{d}y. \tag{25}$$

It is shown from solution (25) that T^S is represented as superposition of localized wave packets, which propagate with the different group velocities and do not interact with each other. This is the property of ballistic heat transport (see, e.g., [46]). In contrast to the infinite chain, the wave packets can propagate both from the boundary (is described by second and third terms in (25)) and toward boundary (is described by first term in 25). The fourth term is equal to zero, because $T^0(-x) = 0$. Using the property of convolutions, we simplify Eq. (25):

$$T^S = \frac{1}{2\pi} \int_0^\pi T^0 \left(|x + v_s t \cos \theta| \right) \mathrm{d}\theta. \tag{26}$$

Remark 1. In [20], the heat transport in the infinite Hooke chain is investigated in the frameworks of both the lattice dynamics approach and the Boltzmann kinetic theory. Following the latter, solution for the continuum kinetic temperature field is derived using the distribution function as solution of the collisionless Boltzmann transport equation. The result coincides with predictions from the lattice dynamics approach. As for the semi-infinite free-end Hooke chain, the kinetic temperature can be obtained in the same way, if the solution of the collisionless Boltzmann transport equation with evenness condition at the boundary ($x = 0$) is known. This approach leads to the same result (Eq. (26)).

3.3 Fast term

Analogously, using assumption (18) with $a\Delta N \ll \mathcal{A}$ and $\Delta N \gg 1$ and (23), we obtain the expression for the fast term T^F. Since the main contribution to the terms T^F comes from points $\theta_1 \approx \theta_2$, as it is shown in Sect. 3.2, $\omega(\theta_1) + \omega(\theta_2) \approx 2\omega(\theta_1)$. According to Sect. 3.2, the fundamental solution, g_c^F, can be written as

$$g_c^F(x, y) = \frac{\delta(x - y) + \delta(x + y)}{2\pi} \int_0^\pi \cos(2\omega(\theta)t) \mathrm{d}\theta = \frac{\delta(x - y) + \delta(x + y)}{2} J_0(4\omega_e t). \tag{27}$$

Then, Eq. for T^F has the form

$$T^F = \frac{T^0(x)H(x) + T^0(-x)H(-x)}{2} J_0(4\omega_e t) = \frac{T^0(x)}{2} J_0(4\omega_e t). \tag{28}$$

Therefore, the expression for the fast term of the kinetic temperature, T^F, coincides with the same expression for the infinite chain [38].

Thus, the final expression for kinetic temperature in the continuum limit (16) is the sum of the contributions T^F, corresponding to the fast processes caused by equilibration of the kinetic and potential energies and T^S, corresponding to the slow processes caused by ballistic heat transport.
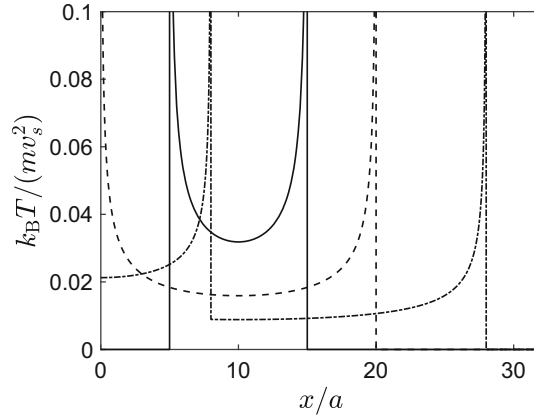
4 Fundamental continuum solution

We consider instantaneous thermal perturbation at some point ha, $h \in \mathbb{N} \cup \{0\}$. The initial temperature profile, corresponding to the considered case, is

$$T^0(x) = A\delta(x - ha), \tag{29}$$

---

[9] Here, evenness property of the Dirac delta function is used.

Fig. 2 Thermal waves at $\omega_e t = 5$ (solid line), $\omega_e t = 10$ (dashed line), $\omega_e t = 18$ (dash-dotted line)

where A is a constant with dimension $K \cdot m$. We write the continuum solution for the kinetic temperature as[10]

$$T \approx T^S = \frac{A}{2\pi} \int_0^\pi \delta(|x + v_s \cos\theta t| - ha)\mathrm{d}\theta. \tag{30}$$

Here, we omit the term T^F because time scale of the fast process is much less than time scale of the ballistic heat transport. Calculation of the integral (30) is carried out using the identity [47]:

$$\int_{\mathcal{D}} \delta(f(\xi))\mathrm{d}\xi = \sum_i |f'(\xi_i)|^{-1}, \qquad f(\xi_i) = 0, \tag{31}$$

where ξ_i are zeros of function f, lying inside the domain $\mathcal{D}$. Therefore, we have the following solution for the kinetic temperature:

$$T(x, t) = \frac{A}{2\pi} \left(\frac{H(v_s t - |x - ha|)}{\sqrt{v_s^2 t^2 - (x - ha)^2}} + \frac{H(v_s t - |x + ha|)}{\sqrt{v_s^2 t^2 - (x + ha)^2}} \right). \tag{32}$$

We have obtained the continuum solution for kinetic temperature in the semi-infinite chain in the case of instantaneous point heat pulse. However, if we consider the infinite chain with heat pulses at the points ha and $-ha$, the obtained continuum solution is the same (it follows from Eq. for T^S in the infinite Hooke chain, see (40)). Therefore, the continuum kinetic temperature field in the semi-infinite Hooke chain with free end and some source *coincides* with the one in the infinite Hooke chain with the same and mirrored sources. The aforesaid rule will be further referred to as a *principle of continuum solution symmetry*. Thus, expression for kinetic temperature is represented as sum of two contributions. The first contribution is the solution for the infinite chain [27,48] and corresponds to the propagating incident waves. The second term corresponds to the wave, reflected from the free boundary. Note that, at times $t < ha/v_s$, heat propagation can be described via the first term in Eq. (32).

We consider the heat perturbation, located at some point from the boundary ($h = 10$). Behavior of thermal waves, propagation of which obeys Eq. (32), is presented in Fig. 2. It is shown in Fig. 2 that the waves in the semi-infinite chain travel in both directions before and after reflection from the boundary. The front instantly changes direction of propagation after the reflection. Specifically, it is shown that the temperature profile is *not symmetric* with respect to the heat source after the reflection.

Thus, we have analytically described a property of the ballistically propagating thermal waves to reflect from free boundaries. The analytical solution, describing propagation of the waves before and after the reflection, is derived. In the next section, we compare the continuum and discrete descriptions of the kinetic temperature field in cases of perturbation on the finite domain.

---

[10] The type of the initial temperature perturbation contradicts with the assumption, made in Sect. 3.1. However, as it is shown below, the continuum solution has the same physical meaning, which is characteristic for one at arbitrary initial temperature profile.
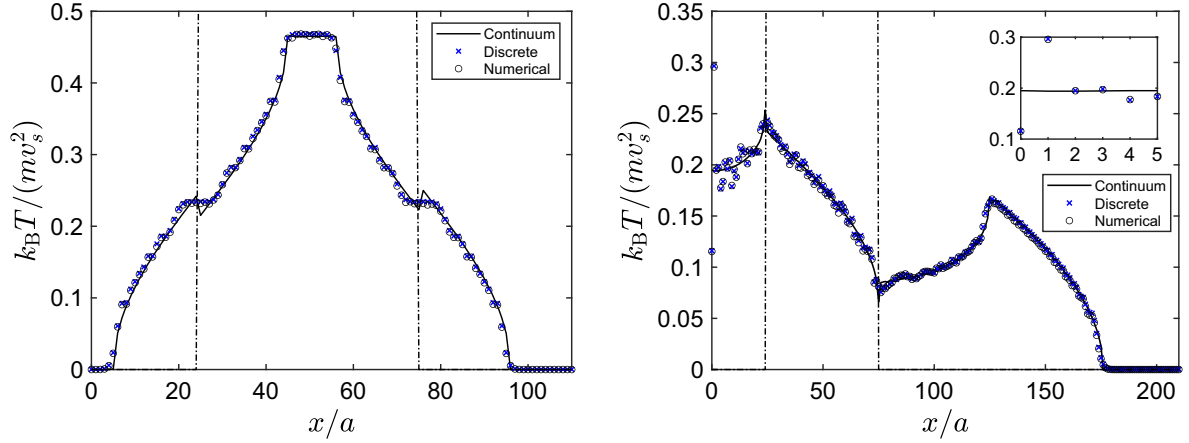
Fig. 3 Discrete and continuum solutions for the kinetic temperature in the semi-infinite free-end Hooke chain in the case of rectangular initial perturbation at $\omega_e t = 20$ (left) and $\omega_e t = 100$ (right). Width of the initial thermal perturbation (34) is limited by the dash-dotted lines

5 Comparison of the discrete and continuum solutions

In this section, evolution of the kinetic temperature fields in the cases of rectangular and step thermal perturbations is under consideration. The initial temperature profiles are chosen for convenience of determination of the characteristic for heat propagation time scales, corresponding to the time for thermal wave to reach the boundary and to reflect from the boundary. We compare the discrete and continuum solutions for kinetic temperature fields and show that the continuum description of heat transport has some restrictions.

In numerical simulations, the kinetic temperature is calculated by its definition (5), where the mathematical expectation is replaced by average over R realizations. To obtain the particle velocity, we solve dynamical Eq. (1) for the finite[11] chain with two free ends with initial conditions[12] (2) and (3) using the fourth-order Candy and Rozmus [49] integrator with the optimizing parameters, proposed in [50] and time step Δt. The following parameters are used:

$$R = 10^5, \qquad \Delta t = 0.01/\omega_e, \tag{33}$$

where ω_e is defined in (1).

5.1 Rectangular initial perturbation

Consider a rectangular heat perturbation, which is defined as

$$k_B T^0(x) = m v_s^2 \left(H(x - L_1) - H(x - L_1 - L_2) \right), \tag{34}$$

where L_1 is a distance from the boundary to the perturbation and L_2 is a width of perturbation. We take $L_1 = 25a$ and $L_2 = 50a$ and the investigate temperature profiles in two cases: before reflection of thermal wave and after the reflection. Discrete and continuum solutions for kinetic temperature are presented in Fig. 3. It is seen in Fig. 3 (left) that the continuum and discrete solutions practically coincide before thermal wave reaches the boundary, except regions near wavefront and near the boundaries of initial perturbation. The mismatches of the discrete and continuum solutions are caused by finiteness of the perturbation length and fast process, which takes place at relatively short times. The discrepancies, mentioned above, become infinitesimal at $\omega_e t = 100$ (Fig. 3, right), when energy of the fast process is much less than the energy transferred along the chain. However, the discrete solution undergoes a jump near the boundary (Fig. 3, inlet). Therefore, the discrete and continuum solutions *disagree* after reflection of thermal wave from the boundary. In order to investigate this jump in detail, we consider behavior of the kinetic temperature at the boundary.

---

[11] Simulations are performed for the chain with 500 particles.
[12] Random numbers ρ_n are uniformly distributed in the segment $[-\sqrt{3}; \sqrt{3}]$, which satisfies condition (4).
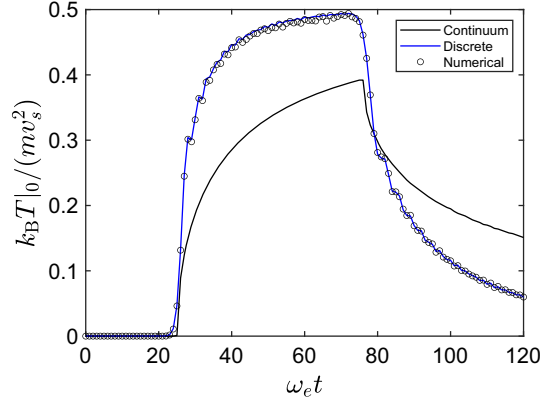
Fig. 4 Evolution of the kinetic temperature at the boundary

The continuum solution for the kinetic temperature at the boundary, $T(0, t)$, has the following form, which can be obtained by substitution of (34) to (16) with $x = 0$ and subsequent integration from 0 to π:

$$k_{\mathrm{B}}T(0, t) = \frac{mv_s^2}{\pi}\left[\arccos\left(\frac{L_1}{v_s t}\right)H\left(t - \frac{L_1}{v_s}\right) - \arccos\left(\frac{L_1 + L_2}{v_s t}\right)H\left(t - \frac{L_1 + L_2}{v_s}\right)\right]. \tag{35}$$

From (35), one can conclude that evolution of the kinetic temperature at the boundary, caused by rectangular perturbation in the chain, has three stages. The first stage is related to fast processes and propagation of thermal waves before reflection ($t < L_1/v_s$). The second stage, related to reflection of thermal wave, begins at $t = L_1/v_s$ and has duration $t = L_2/v_s$. Finally, the third stage begins after reflection of the wave from boundary at $t = (L_1 + L_2)/v_s$ and is related to relaxation of the temperature at the boundary, which decays (according to the continuum solution) as $1/t$. Evolution of the discrete and continuum solutions at the boundary is presented in Fig. 4. One can see from Fig. 4 that the discrete solution for the kinetic temperature at the boundary significantly differs from the continuum one after front reaches the boundary. Growth of the discrete solution at the boundary, caused by reflection of thermal wave and decrease of this, caused by propagation of wavefront backwards, are faster than the same stages of evolution of the continuum solution.

Thus, the process of heat transport in the semi-infinite Hooke chain caused by rectangular perturbation can be generally described by the continuum model, if we deal with the heat propagation far from the boundary. However, there are discrepancies between the continuum and discrete solutions near and at the boundary.

5.2 Step initial perturbation

Consider a step heat perturbation:

$$k_{\mathrm{B}}T^0(x) = mv_s^2 H(L - x), \tag{36}$$

where L is a width of perturbation. The discrete and continuum solutions, corresponding to the case, are presented in Fig. 5 for $L = 50a$.

It is shown in Fig. 5 that the discrete and continuum solutions are also significantly different near the boundary after reflection of thermal wave by virtue of the jump (Fig. 5, inlet). Moreover, some mismatches between the discrete and continuum solutions are observed both before ($t < L/v_s$) and after ($t > L/v_s$) reflection of thermal wave from the boundary. On the one hand, these mismatches could be caused by influence of the fast process, occurring at the same time of the wavefront propagation (Fig. 5, left). On the other hand, however, it is seen from Fig. 5 (right) that the differences between the discrete and continuum solutions remain after the reflection. Indeed, one can see a perturbation, propagating along the chain approximately with the speed of sound, which is described not by the continuum but rather by the discrete solution. An explanation of physical reason of this perturbation is beyond the scope of present paper.

The continuum solution for the kinetic temperature at the boundary can be expressed as

$$k_{\mathrm{B}}T(0, t) = mv_s^2\left(\frac{1}{2}\left(H\left(\frac{L}{v_s} - t\right) + J_0(4\omega_e t)\right) + \frac{1}{\pi}\arcsin\left(\frac{L}{v_s t}\right)H\left(t - \frac{L}{v_s}\right)\right). \tag{37}$$
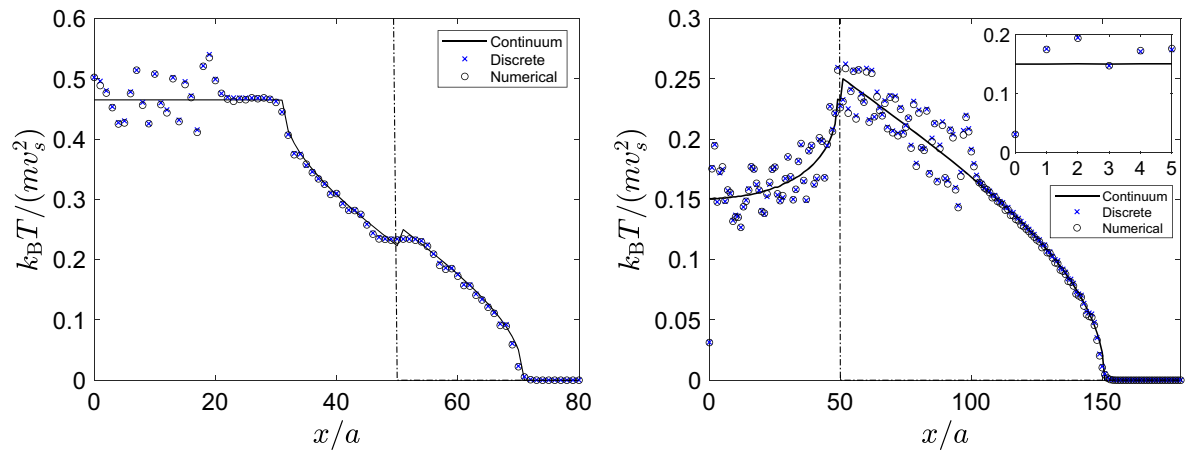
Fig. 5 Discrete and continuum solutions for the kinetic temperature in the semi-infinite free-end Hooke chain in the case of step initial perturbation at $\omega_e t = 20$ (left) and $\omega_e t = 100$ (right). Width of the initial thermal perturbation (36) is limited by the dash-dotted line
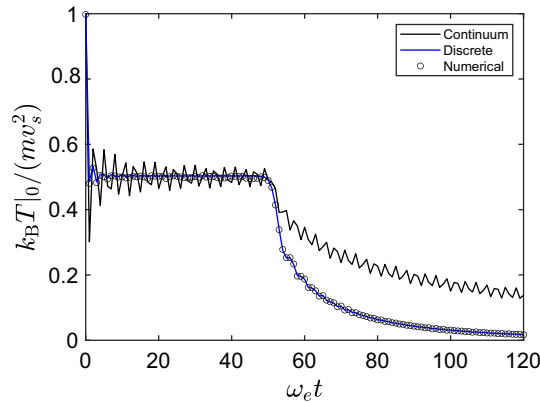
Fig. 6 Evolution of the kinetic temperature at the boundary

The evolution of the kinetic temperature occurs in two stages: equilibration of the kinetic temperature (at times $t < L/v_s$), accompanied by the reflection of thermal wave. At times $(t > L/v_s)$ the wavefront propagates after the reflection. Then, the kinetic temperature at the boundary decays.[13] Evolution of functions of the kinetic temperatures at the boundary is presented in Fig. 6.

It is shown in Fig. 6 behavior of the discrete and continuum kinetic temperature fields is significantly different not only at $t > L/v_s$ (when discrete solution also asymptotically deviates from the continuum) but also at $t < L/v_s$.

Remark 2. According to the preliminary calculations, both discrete and continuum solutions for the kinetic temperature at the boundary are scale invariant with respect to L.[14]

Thus, the continuum solution for kinetic temperature significantly differs from the discrete one, which is shown by a jump of the latter near the boundary. The discrete solution at the boundary decays substantially faster than the continuum one. This observation requires a detailed asymptotic analysis based on the stationary phase method [51,52] and therefore needs a separate investigation, which remains beyond the scope of present paper.

In the next section, we compare the discrete and continuum descriptions of heat transport in the semi-infinite and infinite chains.

---

[13] As in the case of rectangular perturbation, the continuum solution decays also as $1/t$.

[14] i.e., the function $T(t)\big|_0$ at width of the initial thermal perturbation $L + \Delta L$ is equal to $T\left(\frac{L+\Delta L}{L}t\right)\big|_0$ at the width L.
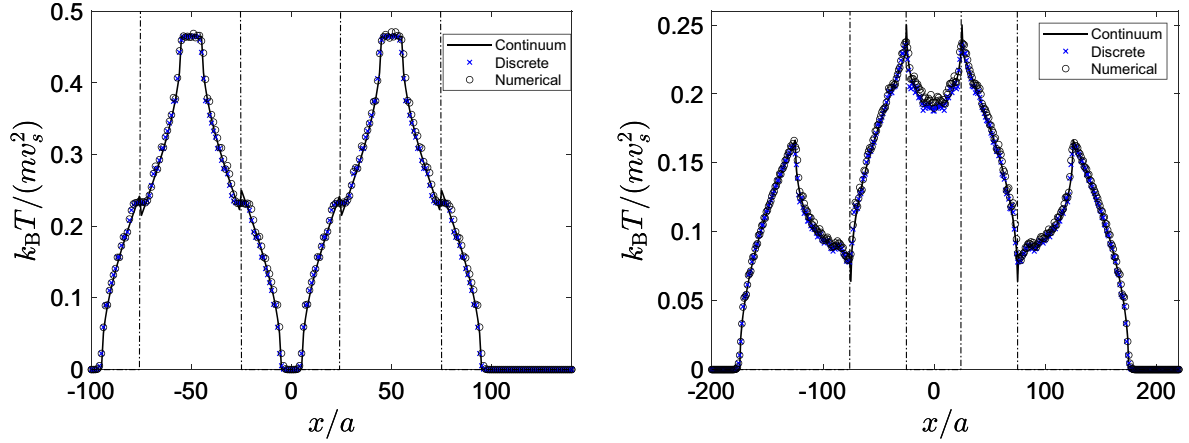
Fig. 7 Discrete and continuum solutions for kinetic temperature in the infinite Hooke chain, in the case of double rectangular initial perturbation (38) at $\omega_e t = 20$ (left) and $\omega_e t = 100$ (right). Width of the initial thermal perturbation (38) is limited by the dash-dotted lines

6 Kinetic temperatures in the infinite chain

In the section, we investigate heat transport in the *infinite* Hooke chain in the case of two symmetric with respect to zero initial thermal perturbations, i.e.,

$$k_{\mathrm{B}}T^0(x) = mv_s^2\Big(H(x - L_1) - H(x - L_1 - L_2) + H(x + L_1 + L_2) - H(x + L_1)\Big), \qquad (38)$$

where the values L_1 and L_2 are defined in Sect. 5.1. The initial temperature profile (38) implies two mirrored with respect to zero heat sources.

Further, we consider the two cases. The first case corresponds to symmetry of heat sources but uncorrelated initial velocities. Therefore, the governing dynamical equations are

$$\ddot{u}_n = \omega_e^2(u_{n+1} - 2u_n + u_{n-1}), \quad n \in \mathbb{Z} \setminus \{0\}. \qquad (39)$$

with initial conditions (2), (3), and (4), corresponding to (38). The problem is solved numerically in the same way as discussed in Sect. 5 and the periodic boundary conditions are used. Analytical solution of the problem is also presented in both the discrete (see Eq. (12)) and continuum descriptions. The continuum solution is proposed in [27,39]:

$$
\begin{aligned}
T_{\inf}(x, t) &= T_{\inf}^F(x, t) + T_{\inf}^S(x, t), \\
T_{\inf}^F &= \frac{T^0(x)}{2} J_0(4\omega_e t), \quad T_{\inf}^S = \frac{1}{2\pi} \int_0^\pi T^0(x + v_s t \cos\theta)\mathrm{d}\theta.
\end{aligned}
\qquad (40)
$$

The discrete and continuum solutions are presented in Fig. 7 for the different moments of time. It is seen from Fig. 7 that the continuum and discrete solutions are in good agreement. Moreover, in the domain $x \geqslant 0$ the continuum kinetic temperature field coincides with the same field in the semi-infinite chain[15]. As expected, the principle of continuum solution, formulated in Sect. 4, is fulfilled. However, the corresponding discrete solutions disagree (Fig. 3, right). The reason of the mismatch is the random initial velocities are uncorrelated. If so, then the discrete solutions are not symmetric with respect to zero even in case of mirrored heat sources.

Consider another case, which is governed by the dynamical Eq. (39) with initial conditions (2). In addition, we require the following condition for random numbers ρ_n:

$$\rho_{-n} = \rho_n, \qquad (41)$$

which implies a symmetry with respect to zero of both initial temperature profile and field of initial velocities simultaneously. To the best of our knowledge, analytical solution for the kinetic temperature (in both the

---

[15] Therefore, before reflection from the boundary, the continuum solution for the kinetic temperature in the semi-infinite chain obeys solution (40).
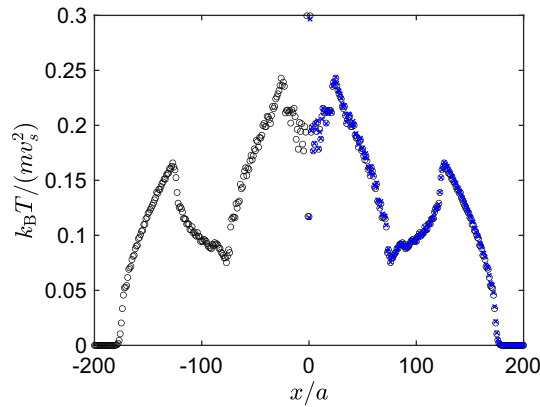
Fig. 8 The discrete (numerical) solution for the kinetic temperature field in the infinite Hooke chain in the case of double rectangular initial perturbation (38) with condition (41) (black circles) and the discrete solution for the kinetic temperature in the semi-infinite free end Hooke chain in the case of rectangular initial perturbation (34) (blue crosses)

discrete and continuum formulations), corresponding to problem (39) with (41) is unknown. Therefore, we calculate numerically the kinetic temperature in the same way as discussed earlier (for the case of uncorrelated initial velocities). Comparison between kinetic temperature field in the considered model at $\omega_e t = 100$ with the corresponding solution for the semi-infinite chain (Eqs. (16) and (11)) is presented in Fig. 8. It is seen from Fig. 8 that the discrete solution for the semi-infinite chain in the case of the rectangular perturbation is the same as solution for the infinite Hooke chain with exactly mirrored heat sources (with symmetric initial velocity fields with respect to zero). Therefore, the discrete solution for kinetic temperature in the semi-infinite Hooke chain with free end and some field of initial velocities coincides with the one in the infinite Hooke chain with the same and mirrored initial velocity fields.

Thus, symmetry of the initial kinetic temperature field (with respect to zero) is enough for symmetry of the continuum solution, but the symmetry of the discrete solution should be in addition provided by the symmetry of the initial velocity field.

7 Conclusions

In the paper, we have investigated the process of unsteady heat transfer in the semi-infinite free end Hooke chain. We have proposed both discrete (exact) and continuum descriptions of this process, studying evolution of the kinetic temperature after an instantaneous heat pulse.

The discrete kinetic temperature field can be constructed by discrete analogue of convolution of the initial temperature profile and the corresponding time derivative of the fundamental solution (see Eqs. (13) and (14)). On the other hand, the solution can be obtained by symmetry property of the kinetic temperature field in the infinite chain with exactly mirrored heat sources (condition (41), implying symmetry of the initial velocity field, is fulfilled). In turn, the continuum solution for the semi-infinite chain coincides with the continuum solution for the infinite chain with mirrored heat sources, corresponding to the initial kinetic temperature field.

It was analytically shown that process of ballistic heat propagation in the chain has at least two transient processes. The first is associated with reflection of thermal wave from the free boundary. The second transient process is related to subsequent propagation of thermal waves backwards. Comparison of the discrete and continuum solutions for the kinetic temperature revealed mismatch between themselves near the boundary and at the boundary during the transient processes. Indeed, the continuum solution does not change in space near the boundary, where the discrete solution undergoes a jump. Based on aforesaid, we conclude that the continuum description (which may be obtained, e.g., from the Boltzmann kinetic theory) of ballistic heat transport in the lattices with boundary conditions needs clarification with taking into account discreteness of the lattices.

The continuum solution can be improved at least in two ways. The first is obtaining large time asymptotics for the discrete solution (either through Eq. (11) in the way, as proposed in [28], or through asymptotic solution of Eq. (14) in the way, as proposed in [53]) and then to proceed to the continuum limit. The second way is to solve heat transport problem in the infinite chain with mirrored with respect to zero fields of initial velocities and then perform a continualization procedure, as proposed either in [20] or in [40]. The improved continuum

solution can be used as the constitutive relation (in particular, for problems of thermoelasticity (see [54]) or thermoelectricity (see, e.g., [55]).

An explanation of mechanism of origin of the kinetic temperature jump near the boundary has not been provided by the model of the semi-infinite chain yet. In order to understand this, heat transport through the boundary of the two chains with significantly different stiffnesses was numerically investigated, analogously as discussed in Sect. 5. In this system, the jump of the kinetic temperature is the Kapitza jump, which was discovered experimentally long time ago [56]. From these observations, one can assume that the jump of the kinetic temperature near the free end is the limiting case of the Kapitza jump in the two interacting chains with equal masses and stiffnesses, ratio of which is infinitesimal. However, this assumption requires a confirmation based on the analytical treatments. The problem, considered and solved in the present paper, can be auxiliary. In general, a problem of heat transport in the heterogeneous lattices is as yet hard to solve analytically but some progress in studying it is attained in both the steady-state [57–59] and non-stationary [53, 60] formulations.

The results of the present paper are expected to be important for comprehensive understanding of unsteady thermal processes in the lattices with free boundaries and thus to development of full-fledged theory of heat transport therein, which can be verified by the experiments, described, e.g., in [9,31–33,61]. However, real systems are generally anharmonic (nonlinear) and therefore investigation of heat propagation therein should take into account nonlinearity. On the other hand, heat transport regime remains quasiballistic in weakly anharmonic lattices at relatively short times and can be therefore qualitatively described in the harmonic approximation (see, e.g., [54,57,62,63]). In particular, it is shown in paper [57] that the jump of the temperature in the neighborhood of isotopic defect is preserved for insufficient time. However, the jump disappears in process of long time owing to nonlinearity. We assume that, depending on width of the initial heat pulse and on distance of the latter from the boundary, the similar effect may be likely observed in the nonlinear semi-infinite lattices.

A Derivation of the discrete analogue of fundamental solution

Here, we derive the discrete fundamental solution, namely $g_{n,j_s}^S(\Delta N)$. Expanding a product of cosines in (17) yields

$$
S_{nj} = \frac{1}{16\pi^2} \iint_{-\pi}^{\pi} \Bigg[\cos((n+j+1)(\theta_1+\theta_2)) + \cos((n+j+1)(\theta_1-\theta_2))
$$
$$
+ \cos((n-j)(\theta_1+\theta_2)) + \cos((n-j)(\theta_1-\theta_2)) + \cos\left(\frac{(2j+1)(\theta_1+\theta_2)}{2} - \frac{(2n+1)(\theta_1-\theta_2)}{2}\right)
$$
$$
+ \cos\left(\frac{(2j+1)(\theta_1+\theta_2)}{2} + \frac{(2n+1)(\theta_1-\theta_2)}{2}\right) + \cos\left(\frac{(2n+1)(\theta_1+\theta_2)}{2} - \frac{(2j+1)(\theta_1-\theta_2)}{2}\right)
$$
$$
+ \cos\left(\frac{(2n+1)(\theta_1+\theta_2)}{2} + \frac{(2j+1)(\theta_1-\theta_2)}{2}\right) \Bigg] \cos\left((\omega(\theta_1)-\omega(\theta_2))t\right) d\theta_1 d\theta_2.
$$

$$(42)$$

Therefore, the expression for $g_{n,j_s}^S(\Delta N)$ can be rewritten as a sum of the following eight terms:

$$
g_{n,j_s}^S(\Delta N) = \frac{1}{16\pi^2 a} \iint_{-\pi}^{\pi} \cos\left((\omega(\theta_1)-\omega(\theta_2))t\right) \sum_{i=1}^{8} \varphi_i(\theta_1,\theta_2) d\theta_1 d\theta_2,
$$

$$
\varphi_1(\theta_1,\theta_2) = \frac{1}{2\Delta N} \sum_{j=j_s-\Delta N+1}^{j_s+\Delta N} \cos\left((n+j+1)(\theta_1+\theta_2)\right)
$$

$$
= \frac{1}{2\Delta N} \cos\left(\frac{3(\theta_1+\theta_2)}{2} + (\theta_1+\theta_2)(n+j_s)\right) \frac{\sin\left((\theta_1+\theta_2)\Delta N\right)}{\sin\left(\frac{\theta_1+\theta_2}{2}\right)},
$$

$$
\varphi_2(\theta_1,\theta_2) = \frac{1}{2\Delta N} \sum_{j=j_s-\Delta N+1}^{j_s+\Delta N} \cos\left((n+j+1)\Delta\theta\right)
$$

$$= \frac{1}{2\Delta N} \cos\left(\left(n + j_s + \frac{3}{2}\right)\Delta\theta\right) \frac{\sin(\Delta N \Delta\theta)}{\sin\frac{\Delta\theta}{2}},$$

$$\varphi_3(\theta_1, \theta_2) = \frac{1}{2\Delta N} \sum_{j=j_s-\Delta N+1}^{j_s+\Delta N} \cos((n-j)(\theta_1+\theta_2))$$

$$= \frac{1}{2\Delta N} \cos\left((\theta_1+\theta_2)\left(\frac{1}{2}+j_s-n\right)\right) \frac{\sin((\theta_1+\theta_2)\Delta N)}{\sin\left(\frac{\theta_1+\theta_2}{2}\right)},$$

$$\varphi_4(\theta_1, \theta_2) = \frac{1}{2\Delta N} \sum_{j=j_s-\Delta N+1}^{j_s+\Delta N} \cos((n-j)\Delta\theta)$$

$$= \frac{1}{2\Delta N} \cos\left(\Delta\theta\left(\frac{1}{2}+j_s-n\right)\right) \frac{\sin(\Delta N \Delta\theta)}{\sin\frac{\Delta\theta}{2}},$$

$$\varphi_5(\theta_1, \theta_2) = \frac{1}{2\Delta N} \sum_{j=j_s-\Delta N+1}^{j_s+\Delta N} \cos\left(\frac{(2j+1)(\theta_1+\theta_2)}{2} - \frac{(2n+1)(\theta_1-\theta_2)}{2}\right)$$

$$= \frac{1}{2\Delta N} \cos\left(\theta_1\left(\frac{1}{2}+j_s-n\right) + \theta_2\left(\frac{3}{2}+j_s+n\right)\right) \frac{\sin((\theta_1+\theta_2)\Delta N)}{\sin\left(\frac{\theta_1+\theta_2}{2}\right)},$$

$$\varphi_6(\theta_1, \theta_2) = \frac{1}{2\Delta N} \sum_{j=j_s-\Delta N+1}^{j_s+\Delta N} \cos\left(\frac{(2j+1)(\theta_1+\theta_2)}{2} + \frac{(2n+1)(\theta_1-\theta_2)}{2}\right)$$

$$= \frac{1}{2\Delta N} \cos\left(\theta_2\left(\frac{1}{2}+j_s-n\right) + \theta_1\left(\frac{3}{2}+j_s+n\right)\right) \frac{\sin((\theta_1+\theta_2)\Delta N)}{\sin\left(\frac{\theta_1+\theta_2}{2}\right)},$$

$$\varphi_7(\theta_1, \theta_2) = \frac{1}{2\Delta N} \sum_{j=j_s-\Delta N+1}^{j_s+\Delta N} \cos\left(\frac{(2n+1)(\theta_1+\theta_2)}{2} - \frac{(2j+1)(\theta_1-\theta_2)}{2}\right)$$

$$= \frac{1}{2\Delta N} \cos\left(\theta_1\left(\frac{1}{2}+j_s-n\right) - \theta_2\left(\frac{3}{2}+j_s+n\right)\right) \frac{\sin(\Delta N \Delta\theta)}{\sin\left(\frac{\Delta\theta}{2}\right)},$$

$$\varphi_8(\theta_1, \theta_2) = \frac{1}{2\Delta N} \sum_{j=j_s-\Delta N+1}^{j_s+\Delta N} \cos\left(\frac{(2n+1)(\theta_1+\theta_2)}{2} + \frac{(2j+1)(\theta_1-\theta_2)}{2}\right)$$

$$= \frac{1}{2\Delta N} \cos\left(\theta_2\left(\frac{1}{2}+j_s-n\right) - \theta_1\left(\frac{3}{2}+j_s+n\right)\right) \frac{\sin(\Delta N \Delta\theta)}{\sin\left(\frac{\Delta\theta}{2}\right)}, \quad \Delta\theta = \theta_1 - \theta_2. \tag{43}$$

We rewrite the components φ_2, φ_4, φ_7, φ_8, containing the difference of wave numbers $\Delta\theta$ as follows:

$$\varphi_2 = \frac{\Delta\theta}{2}\left[\frac{\cos\frac{3\Delta\theta}{2}}{\sin\frac{\Delta\theta}{2}}(\cos((n+j_s)\Delta\theta)) - \frac{\sin\frac{3\Delta\theta}{2}}{\sin\frac{\Delta\theta}{2}}(\sin((n+j_s)\Delta\theta))\right]\mathrm{sinc}(\Delta N \Delta\theta),$$

$$\mathrm{sinc}(x) = \frac{\sin x}{x},$$

$$\varphi_4 = \frac{\Delta\theta}{2}\left[\cot\frac{\Delta\theta}{2}\cos((n-j_s)\Delta\theta) + \sin((n-j_s)\Delta\theta)\right]\mathrm{sinc}(\Delta N \Delta\theta),$$

$$\varphi_7 = \frac{\Delta\theta}{2}\left[\frac{\cos\frac{3\Delta\theta}{2}}{\sin\frac{\Delta\theta}{2}}\cos(\Delta\theta(n+j_s) - \theta_1(2n+1)) - \frac{\sin\frac{3\Delta\theta}{2}}{\sin\frac{\Delta\theta}{2}}\sin(\Delta\theta(n+j_s) - \theta_1(2n+1))\right] \tag{44}$$

$$\mathrm{sinc}(\Delta N \Delta\theta),$$

$$\varphi_8 = \frac{\Delta\theta}{2}\left[\cot\frac{\Delta\theta}{2}\cos(\theta_1(2n+1) - \Delta\theta(n-j_s)) - \sin(\theta_1(2n+1) - \Delta\theta(n-j_s))\right]$$

$$\mathrm{sinc}(\Delta N \Delta\theta).$$

Equation (44) can be simplified due to our assumptions about continualization (see Sect. 3.1). For $\Delta N \gg 1$, the function $\mathrm{sinc}(x)$ is equal to 1 if $\Delta\theta$ is zero and fast tends to zero if $\Delta\theta$ is not equal to zero. Therefore, the main contribution to the function $g_{n,j_s}^S(\Delta N)$ comes from two close wavenumbers θ_1, θ_2. Therefore, in the

limit cases of $\Delta\theta \to 0$ and $\Delta N \gg 1$, we have

$$
\begin{aligned}
\varphi_2 &= \cos\left((n + j_s)\Delta\theta\right)\operatorname{sinc}(\Delta N\Delta\theta) + O\left(\frac{1}{\Delta N}\right), \\
\varphi_4 &= \cos\left((n - j_s)\Delta\theta\right)\operatorname{sinc}(\Delta N\Delta\theta) + O\left(\frac{1}{\Delta N}\right), \\
\varphi_7 &= \cos(\theta_1(2n + 1) - (n + j_s)\Delta\theta)\operatorname{sinc}(\Delta N\Delta\theta) + O\left(\frac{1}{\Delta N}\right), \\
\varphi_8 &= \cos(\theta_1(2n + 1) - (n - j_s)\Delta\theta)\operatorname{sinc}(\Delta N\Delta\theta) + O\left(\frac{1}{\Delta N}\right), \\
\varphi_1 &= \varphi_3 = \varphi_5 = \varphi_6 = O\left(\frac{1}{\Delta N}\right).
\end{aligned}
\tag{45}
$$

The difference $\omega(\theta_1) - \omega(\theta_2)$ can be decomposed into series:

$$
\omega(\theta_1) - \omega(\theta_2) \approx \omega'(\theta_1)\Delta\theta.
\tag{46}
$$

Substitution of (45), (46) to (43) with dropping out of the terms of order $O\left(\frac{1}{\Delta N}\right)$ gives the expression (19).

B Derivation of expressions for wave packets in the limit of mesoscale

We show that approximation of expressions for wave packets in (20) in the limit case ($\Delta N \gg 1$) approaches us to the Fourier transform of the sinc function. Indeed,

$$
\begin{aligned}
\frac{1}{2\pi a} \int_{\theta-\pi}^{\theta+\pi} \cos\left(q\,\Xi\right)\operatorname{sinc}(q\,\Delta N)\mathrm{d}q &= \frac{1}{2\pi a\Delta N} \int_{(\theta-\pi)\Delta N}^{(\theta+\pi)\Delta N} \cos\left(\frac{q\,\Xi}{\Delta N}\right)\operatorname{sinc} q\,\mathrm{d}q \\
&\approx \frac{1}{2\pi a\Delta N} \int_{-\infty}^{\infty} \cos\left(\frac{q\,\Xi}{\Delta N}\right)\operatorname{sinc} q\,\mathrm{d}q = \operatorname{Re}\left(\frac{1}{2\pi a\Delta N} \int_{-\infty}^{\infty} e^{\mathrm{i}\left(\frac{q\,\Xi}{\Delta N}\right)}\operatorname{sinc} q\,\mathrm{d}q\right).
\end{aligned}
\tag{47}
$$

Analogously,

$$
\frac{1}{2\pi a} \int_{\theta-\pi}^{\theta+\pi} \sin\left(q\,\Xi\right)\operatorname{sinc}(q\,\Delta N)\mathrm{d}q \approx \operatorname{Im}\left(\frac{1}{2\pi a\Delta N} \int_{-\infty}^{\infty} e^{\mathrm{i}\left(\frac{q\,\Xi}{\Delta N}\right)}\operatorname{sinc} q\,\mathrm{d}q\right).
\tag{48}
$$

Since

$$
\frac{1}{2\pi} \int_{-\infty}^{\infty} e^{\mathrm{i}\xi q}\operatorname{sinc} q\,\mathrm{d}q = \frac{1}{2}H\left(1 - |\xi|\right),
\tag{49}
$$

then one gets

$$
\begin{aligned}
\frac{1}{2\pi a\Delta N} \int_{-\infty}^{\infty} \cos\left(\frac{q\,\Xi}{\Delta N}\right)\operatorname{sinc} q\,\mathrm{d}q &= \frac{1}{2a\Delta N}H\left(1 - \frac{|\Xi|}{\Delta N}\right), \\
\frac{1}{2\pi a\Delta N} \int_{-\infty}^{\infty} \sin\left(\frac{q\,\Xi}{\Delta N}\right)\operatorname{sinc} q\,\mathrm{d}q &= 0.
\end{aligned}
\tag{50}
$$

References

1. Rickert, W., Vilchevskaya, E.N., Müller, W.H.: A note on Couette flow of micropolar fluids according to Eringen's theory. Math. Mech. Complex Syst. **7**, 25–50 (2019). https://doi.org/10.2140/MEMOCS.2019.7.25
2. Rieder, Z., Lebowitz, J.L., Lieb, E.: Properties of a harmonic crystal in a stationary nonequilibrium state. J. Math. Phys. **8**(5), 1073–1078 (1967). https://doi.org/10.1063/1.1705319
3. Lepri, S., Livi, R., Politi, A.: Thermal conduction in classical low-dimensional lattices. Phys. Rep. **377**(1), 1–80 (2003). https://doi.org/10.1016/S0370-1573(02)00558-6
4. Dhar, A.: Heat transport in low-dimensional systems. Adv. Phys. **57**(5), 457–537 (2008). https://doi.org/10.1080/00018730802538522

5. Chang, C.W.: Experimental probing of non-Fourier thermal conductors. In: Lepri, S. (ed.) Thermal Transport in Low Dimensions From Statistical Physics to Nanoscale Heat Transfer, vol. 921, pp. 305–338. Springer, Heidelberg (2016)

6. Huberman, S., Duncan, R.A., Chen, K., Song, B., Chiloyan, V., Ding, Z., Maznev, A.A., Chen, G., Nelson, K.A.: Observation of second sound in graphite at temperatures above 100 k. Science **364**(6438), 375–379 (2019). https://doi.org/10.1126/science.aav3548

7. Johnson, J.A., Maznev, A.A., Cuffe, J., Eliason, J.K., Minnich, A.J., Kehoe, T., Clivia, M., Torres, S., Chen, G., Nelson, K.A.: Direct measurement of room-temperature nondiffusive thermal transport over micron distances in a silicon membrane. Phys. Rev. Lett. **110**, 025901 (2013). https://doi.org/10.1103/PhysRevLett.110.025901

8. Anufriev, R., Gluchko, S., Volz, S., Nomura, M.: Quasi-ballistic heat conduction due to levy phonon flights in silicon nanowires. ACS Nano **12**(12), 11928–11935 (2018). https://doi.org/10.1021/acsnano.8b07597

9. Anufriev, R., Gluchko, S., Volz, S., Nomura, M.: Probing ballistic thermal conduction in segmented silicon nanowires. Nanoscale **11**(28), 13407–13414 (2019). https://doi.org/10.1039/C9NR03863A

10. Chang, C.W., Okawa, D., Garcia, H., Majumdar, A., Zettl, A.: Breakdown of Fouriers law in nanotube thermal conductors. Phys. Rev. Lett. **101**, 075903 (2008). https://doi.org/10.1103/PhysRevLett.101.075903

11. Xu, X., Wang, Yu., Zhang, K.: Length-dependent thermal conductivity in suspended single-layer graphene. Nat. Commun. **5**, 1–6 (2014). https://doi.org/10.1038/ncomms4689

12. Li, N., Ren, J., Wang, L., Zhang, G., Hänggi, P., Li, B.: Colloquium: phononics: manipulating heat flow with electronic analogs and beyond. Rev. Mod. Phys. **84**, 1045–1066 (2012). https://doi.org/10.1103/RevModPhys.84.1045

13. Shahil, K.M., Balandin, A.A.: Thermal properties of graphene and multilayer graphene: applications in thermal interface materials. Solid State Commun. **152**(15), 1331–1340 (2012). https://doi.org/10.1016/j.ssc.2012.04.034

14. Malik, F.K., Fobelets, K.: A review of thermal rectification in solid-state devices. J. Semicond. **43**(10), 1–18 (2022). https://doi.org/10.1088/1674-4926/43/10/103101

15. Dwivedi, N., Ott, A.K.: Graphene overcoats for ultra-high storage density magnetic media. Nat. Commun. **12**, 1–13 (2021)

16. Moore, A.L., Shi, L.: Emerging challenges and materials for thermal management of electronics. Mater. Today **17**(4), 163–174 (2014). https://doi.org/10.1016/j.mattod.2014.04.003

17. Majumdar, A.: Microscale heat conduction in dielectric thin films. J. Heat Transf. **115**(1), 7–16 (1993). https://doi.org/10.1115/1.2910673

18. Cahill, D.G., Ford, W.K., Goodson, K.E., Mahan, G.D., Majumdar, A., Maris, H.J., Merlin, R., Phillpot, S.R.: Nanoscale thermal transport. J. Appl. Phys. **93**(73), 793–818 (2003). https://doi.org/10.1063/1.1524305

19. Spohn, H.: The phonon Boltzmann equation, properties and link to weakly anharmonic lattice dynamics. J. Stat. Phys. **124**, 1041–1104 (2006). https://doi.org/10.1007/s10955-005-8088-5

20. Kuzkin, V.A., Krivtsov, A.M.: Unsteady ballistic heat transport: linking lattice dynamics and kinetic theory. Acta Mech. **232**, 1983–1996 (2021). https://doi.org/10.1007/s00707-020-02927-w

21. Klein, G., Prigogine, I.: Sur la mecanique statistique des phenomenes irreversibles III. Physica **19**(1–12), 1053–1071 (1953). https://doi.org/10.1016/S0031-8914(53)80120-5

22. Schrödinger, E.: Zur Dynamik elastisch gekoppelter Punktsysteme. Ann. Phys. **349**(14), 916–944 (1914). https://doi.org/10.1002/andp.19143491405

23. Muhlich, U., Abali, B.E., dell'Isola, F.: Commented translation of Erwin Schrödinger's paper 'On the dynamics of elastically coupled point systems' (Zur Dynamik elastisch gekoppelter Punktsysteme). Math. Mech. Solids **26**(1), 133–147 (2020). https://doi.org/10.1177/1081286520942955

24. Krivtsov, A.M.: Dynamics of matter and energy. ZAMM (2022). https://doi.org/10.1002/zamm.202100496

25. Hemmer, P.C.: Dynamic and stochastic types of motion in the linear chain. Norges tekniske hoiskole (1959)

26. Krivtsov, A.M.: Heat transfer in infinite harmonic one dimensional crystals. Dokl. Phys. **60**(9), 407–411 (2015). https://doi.org/10.1134/S1028335815090062

27. Sokolov, A.A., Müller, W.H., Porubov, A.V., Gavrilov, S.N.: Heat conduction in 1d harmonic crystal: discrete and continuum approaches. Int. J. Heat Mass Transf. **176**, 121442 (2021). https://doi.org/10.1016/j.ijheatmasstransfer.2021.121442

28. Gavrilov, S.N.: Discrete and continuum fundamental solutions describing heat conduction in a 1d harmonic crystal: discrete-to-continuum limit and slow-and-fast motions decoupling. Int. J. Heat Mass Transf. **194**, 123019 (2022). https://doi.org/10.1016/j.ijheatmasstransfer.2022.123019

29. Guzev, M.A., Sadovskii, V.M., Qi, C.: Inhomogeneous distribution of thermal characteristics in harmonic crystal. In: Indeitsev, D., Krivtsov, A. (eds.) Advanced Problems in Mechanics. APM 2019. Lecture Notes in Mechanical Engineering, pp. 124–138. Springer, Cham (2020)

30. Gudimenko, A.I.: Heat flow in a one-dimensional semi-infinite harmonic lattice with an absorbing boundary. Dal'nevostochnyi Matematicheskii Zhurnal **20**(1), 38–51 (2020). https://doi.org/10.47910/FEMJ202004. (**in Russian**)

31. Northrop, G.A., Wolfe, J.P.: Ballistic phonon imaging in germanium. Phys. Rev. B **22**(12), 6196–6217 (1980). https://doi.org/10.1103/PhysRevB.22.6196

32. Northrop, G.A., Wolfe, J.P.: Phonon imaging: theory and applications. In: Bron, W.E. (ed.) Nonequilibrium Phonon Dynamics, pp. 165–242. Nato ASI Subseries B, Les Arcs (1985)

33. Ravichandran, N.K., Zhang, H., Minnich, A.J.: Spectrally resolved specular reflections of thermal phonons from atomically rough surfaces. Phys. Rev. X **8**(4), 1–11 (2018). https://doi.org/10.1103/PhysRevX.8.041004

34. Krivtsov, A.M., Kuzkin, V.A.: Discrete and continuum thermomechanics. In: Altenbach, H., Öchsner, A. (eds.) Encyclopedia of Continuum Mechanics, pp. 1–16. Springer, Germany (2018)

35. Landau, L.D., Lifshitz, E.M.: Statistical Physics. Pergamon Press, Oxford (1958)

36. Casas-Vázquez, J., Jou, D.: Temperature in nonequilibrium states: a review of open problems and current proposals. Rep. Prog. Phys. **66**(11), 1937–2023 (2003). https://doi.org/10.1088/0034-4885/66/11/R03

37. Puglisi, A., Sarracino, A., Vulpiani, A.: Temperature in and out of equilibrium: a review of concepts, tools and attempts. Phys. Rep. **709**, 1–60 (2017). https://doi.org/10.1016/j.physrep.2017.09.001

38. Krivtsov, A.M.: Energy oscillations in a one-dimensional crystal. Dokl. Phys. **59**(9), 427–430 (2014). https://doi.org/10.1134/S1028335814090080

39. Kuzkin, V.A., Krivtsov, A.M.: Fast and slow thermal processes in harmonic scalar lattices. J. Phys. Condens. Matter **29**, 505401 (2017). https://doi.org/10.1088/1361-648X/aa98eb
40. Gavrilov, S.N., Krivtsov, A.M., Tsvetkov, D.V.: Heat transfer in a one-dimensional harmonic crystal in a viscous environment subjected to an external heat supply. Contin. Mech. Thermodyn. **31**(1), 255–272 (2018). https://doi.org/10.1007/s00161-018-0681-3
41. Takizawa, E., Kobayasi, K.: On the stochastic types of motion in a system of linear harmonic oscillators. Chin. J. Phys. **6**(1), 39–66 (1968)
42. Lee, K.H.: Dynamics of harmonically bound semi-infinite and infinite chains with friction and applied forces. J. Math. Phys. **13**, 1312–1315 (1972). https://doi.org/10.1063/1.1666137
43. Lee, K.H., Kim, H.: Exact solutions for dynamics of finite, semi-infinite, and infinite chains with general boundary and initial conditions. J. Chem. Phys. **57**(12), 5037–5044 (1972). https://doi.org/10.1063/1.1678186
44. Ahmed, H., Nataryan, T., Rao, K.R.: Discrete cosine transform. IEEE Trans. Comput. **100**(1), 90–93 (1974). https://doi.org/10.1109/T-C.1974.223784
45. Vladimirov, V.: Equations of Mathematical Physics. Marcel Dekker, New York (1971)
46. Shi, L.: Nonresistive heat transport by collective phonon flow. Science **364**(6438), 332–333 (2019). https://doi.org/10.1126/science.aax2319
47. Gelfand, I., Shilov, G.: Generalized Functions. Properties and Operations. Academic Press, New York (1964)
48. Allen, P.B., Nghiem, N.A.: Heat pulse propagation and nonlocal phonon heat transport in one-dimensional harmonic chains. Phys. Rev. B **105**, 174302 (2022). https://doi.org/10.1103/PhysRevB.105.174302
49. Candy, J., Rozmus, W.: A symplectic integration algorithm for separable Hamiltonian functions. J. Comput. Phys. **92**(1), 230–256 (1991). https://doi.org/10.1016/0021-9991(91)90299-Z
50. McLachlan, R.I., Atela, P.: The accuracy of symplectic integrators. Nonlinearity **5**(2), 541–562 (1992). https://doi.org/10.1088/0951-7715/5/2/011
51. Erdelyi, A.: Asymptotic Expansions. Courier Corporation, New York (1956)
52. Fedoryuk, M.: The Saddle-Point Method. Nauka, Moscow (1977)
53. Shishkina, E.V., Gavrilov, S.N.: Unsteady ballistic heat transport in a 1d harmonic crystal due to a source on an isotopic defect. arXiv:2206.08079 (2022)
54. Kuzkin, V.A., Krivtsov, A.M.: Ballistic resonance and thermalization in Fermi-Pasta-Ulam-Tsingou chain at finite temperature. Phys. Rev. E **101**, 042209 (2020). https://doi.org/10.1103/PhysRevE.101.042209
55. Ivanova, E.A.: Modeling of thermal and electrical conductivities by means of a viscoelastic Cosserat continuum. Contin. Mech. Thermodyn. **34**, 555–586 (2022). https://doi.org/10.1007/s00161-021-01071-7
56. Kapitza, P.L.: The study of heat transfer in helium II. J. Phys. USSR **4**(181), 114–153 (1941)
57. Gendelman, O.V., Jithu, P.: Kapitza thermal resistance in linear and nonlinear chain models: isotopic defect. Phys. Rev. E **103**, 052113 (2021)
58. Jithu, P., Gendelman, O.V.: Kapitza resistance at a domain boundary in linear and nonlinear chains. Phys. Rev. E **104**, 054119 (2021)
59. Hu, R., Dai, J., Tian, Z.T.: Introduction to the atomistic green's function approach: application to nanoscale phonon transport. In: Liao, B. (ed.) Nanoscale Energy Transport: Emerging Phenomena, Methods and Applications, pp. 1–26. IOP Publishing, Bristol (2020)
60. Tian, Z.T., White, B.E., Jr., Sun, Y.: Phonon wave-packet interference and phonon tunneling based energy transport across nanostructured thin films. Appl. Phys. Lett. **96**(26), 263113 (2010). https://doi.org/10.1063/1.3458831
61. Qu, X., Gu, J.: Phonon transport and thermal conductivity of diamond superlattice nanowires: a comparative study with SiGe superlattice nanowires. RSC Adv. **10**(3), 1243–1248 (2020). https://doi.org/10.1039/C9RA08520C
62. Korznikova, E.A., Kuzkin, V.A., Krivtsov, A.M., Xiong, Daxing, Gani, Vakhid A., Kudreyko, A.A., Dmitriev, S.V.: Equilibration of sinusoidal modulation of temperature in linear and nonlinear chains. Phys. Rev. E **102**, 062148 (2020). https://doi.org/10.1103/PhysRevE.102.062148
63. Liazhkov, S.D., Kuzkin, V.A.: Unsteady two-temperature heat transport in mass-in-mass chains. Phys. Rev. E **105**, 054145 (2022). https://doi.org/10.1103/PhysRevE.105.054145